electronic reprint

Journal of
Applied Crystallography
ISSN 0021-8898
Editor: **Gernot Kostorz**

Quantitative Rietveld texture analysis of zirconium from single synchrotron diffraction images

Gloria Ischia, Hans-Rudolf Wenk, Luca Lutterotti and Florian Berberich

Journal of
Applied Crystallography
ISSN 0021-8898

Received 8 September 2004
Accepted 24 February 2005

Quantitative Rietveld texture analysis of zirconium from single synchrotron diffraction images

Gloria Ischia,[a,b] Hans-Rudolf Wenk,[a,c]* Luca Lutterotti[b] and Florian Berberich[d]

[a]Department of Earth and Planetary Science, University of California, Berkeley CA 94720, USA, [b]Dipartimento di Ingegneria dei Materiali, Università Trento, Italy, [c]GeoForschungsZentrum Potsdam, Germany, and [d]European Synchrotron Radiation Facility, Grenoble, France. Correspondence e-mail: wenk@seismo.berkeley.edu

Preferred orientation is immediately visible on synchrotron diffraction images as intensity variations along Debye rings. In this report, the Rietveld method is applied to obtain quantitative information about the orientation distribution from the analysis of a single synchrotron diffraction image. The method is illustrated for hexagonal cold-rolled zirconium, investigated *in situ* in a vacuum furnace with high-energy X-rays, both before and after the onset of recrystallization.

1. Introduction

With CCD cameras and image-plate recorders, synchrotron diffraction images are increasingly used to document the presence of texture in a wide variety of materials, including metals (Bäckstrøm *et al.*, 1996; Puig-Molina *et al.*, 2003), minerals (Heidelbach *et al.*, 1999; Wenk, Lonardelli *et al.*, 2004) and biological samples (Wenk & Heidelbach, 1998; Lonardelli *et al.*, 2005). While the presence of texture is immediately obvious, only a detailed analysis provides information about the orientation distribution function (ODF). In much of the earlier work on this subject, texture information was obtained by imposing axial sample symmetry, by combining images obtained in different sample orientations, or by rotating the sample during an exposure (Bunge *et al.*, 2003; Skrotzki *et al.* 2003). These methods are cumbersome and often not possible owing to geometric constraints or if the sample undergoes changes with time. Thus, a method that relies on single images would be highly desirable. Indeed, it has recently been shown that intensity variations along several Debye rings contain sufficient information to determine the ODF, without imposing any sample symmetry, both for cubic and for hexagonal materials (Puig-Molina *et al.*, 2003; Wenk & Grigull, 2003). Intensity variations along Debye rings were extracted from the images and used for texture computation. In this report, we are advancing the approach by applying the Rietveld method directly to two-dimensional images, such as those shown in Fig. 1 for rolled and recrystallized zirconium.

2. Experimental technique

The sample used in this study was a 1 mm thick sheet of cold-rolled zirconium. Measurements were carried out at the ESRF in Grenoble on the high-energy beamline ID15B *in situ* in a vacuum furnace, as described by Puig-Molina *et al.* (2003). The sample was analyzed in transmission with a monochromatic X-ray beam of wavelength 0.138 Å and size 0.2 × 0.2 mm. The beam direction was orthogonal to the rolling plane. Data were recorded with a 1242 × 1152 CCD camera placed behind the sample, at a distance of 325 mm, also orthogonal to the beam direction. Exposure times were 1 s. We selected two images from a systematic study of recrystallization and phase transformations to illustrate the method. The first image was collected at room temperature (Fig. 1*a*), the second at 833 K (Fig. 1*b*). In the image of the recrystallized sample individual grains are clearly visible.

3. Data analysis

For the texture analysis we relied on the Rietveld method as implemented in the *MAUD* (material analysis using diffraction) software package (Lutterotti *et al.*, 1997). A new feature of this program is that images in TIFF format (or corresponding ESRF and APS formats), without previous processing, *e.g.* in *FIT2D* (Hammersley, 1998), can be entered directly (Lonardelli *et al.*, 2005). The 16 bit CCD image is used to obtain spectra integrated over azimuthal increments. The user needs to determine an approximate image center on the graphics screen, which will later be refined in the Rietveld procedure. Here, the full 360° image has been integrated over 5° into 72 slices for the room-temperature image and over 15° into 24 slices for the 833 K image in order to obtain better grain statistics. The integrated slices are then used as spectra by the program. In transmission geometry and for short wavelengths the pole-figure coverage corresponds to a circle near the periphery of the pole-figure coverage.

The steps used in the Rietveld refinement were as follows.

(i) Refinement of background parameters of spectra and center of the two-dimensional image. We used three background parameters that define a polynomial. Because of the radial homogeneity of the background on these particular images, it was sufficient to refine the background parameters for the whole image rather than for each individual spectrum. Table 1 verifies that the results are very similar for three parameters rather than $3 \times 72 = 216$ and $3 \times 24 = 72$. If the background varies with azimuth (*e.g.* because of shadows in high-pressure cells), the background has to be refined for each spectrum.

(ii) Refinement of previous parameters plus lattice parameters, crystallite size, microstrain and displacement parameter.

(iii) Refinement of all previous parameters plus texture. A modified WIMV (Matthies & Vinel, 1982) algorithm, capable of processing irregular and incomplete pole coverage (EWIMV), was used to calculate the ODF. A $10 \times 10 \times 10°$ grid was applied for the computation of the ODF, and the tube projection technique (Pawlik, 1986) was used to account for the low experimental pole-figure coverage. A projection tube radius of 20° was chosen. With 24

Table 1
Quantitative texture information for zirconium, measured under different conditions (RT is room temperature, m.r.d. is multiples of a random distribution), particularly using different numbers of background parameters (bp) as discussed in the text.

		Synchrotron RT		Synchrotron 833 K	
	Pole-figure goniometer	3 bp	216 bp	3 bp	72 bp
(0001) max (m.r.d.)	9.7	10.4	10.6	7.4	8.9
$(10\bar{1}0)$ max (m.r.d.)	5.4	9.7	9.9	4.2	4.4
$(11\bar{2}0)$ max (m.r.d.)	3.0	4.5	4.4	3.8	3.6

reflections used, this setup assured adequate formal coverage of the ODF, with solutions for all cells.

The discrete ODF, interpolated into a 5° grid, was exported from *MAUD* and used as input in *BEARTEX* (Wenk *et al.*, 1998), where the ODF was smoothed with a 7.5° filter to eliminate stochastic effects, and from this ODF pole figures were recalculated.

4. Results

The refinement succeeded without complications. Texture results are displayed as (0001), $(10\bar{1}0)$ and $(11\bar{2}0)$ pole figures that were recalculated from the ODF (Fig. 2). The same logarithmic contour scale is used for all. As is apparent, the texture is very strong. The synchrotron Rietveld pole figures (Figs. 2*b* and 2*c*) are compared with pole figures derived from conventional measurements of the room-temperature sample with a pole-figure goniometer (Fig. 2*a*). In that case, three pole figures were measured in reflection geometry to a maximum pole distance of 80°.

5. Discussion

Figs. 2(*a*) and 2(*b*) compare recalculated pole figures obtained on the same sample with a pole-figure goniometer and measured for several hours with those derived from a synchrotron image measured in 1 s. The resemblance is striking, especially considering the minimal coverage in the case of the synchrotron pole figure. The pole-figure goniometer pole figures are more symmetrical than the synchrotron pole figures. This difference can be explained by the inferior grain statistics in the latter case. It should be noted that most of the high pole density regions in the pole figures, particularly the (0001) maximum near the normal direction, were not covered by measurements but are inferred from the ODF. Overall, the comparison is very good, with almost identical pole density values (Table 1). The largest deviations are in exaggerated pole densities for the synchrotron (0001) and $(10\bar{1}0)$ pole figures near the periphery, corresponding to the actual measured data.

For us it was even more surprising that results from a spotty diffraction pattern of the high-temperature sample, which we would have deemed impossible to analyze, provided convincing results. All pole figures display more or less orthorhombic symmetry, consistent with the deformation conditions.

The dominant texture feature is a (0001) double maximum around the normal direction and extended towards the transverse direction; moreover, there is a $(10\bar{1}0)$ maximum in the rolling direction at room temperature (Figs. 2*a* and 2*b*). This is consistent with other studies of zirconium (*e.g.* Wenk, Lonardelli & Williams, 2004). The *in situ* synchrotron study documents for zirconium an onset of recrystallization at 773 K, as evidenced by a spot pattern (Fig. 1*b*). At 833 K (and for a few minutes later), recrystallization is already very advanced, with minimal continuous intensity remaining. The recrystallization texture is similar to that at room temperature. The double maximum for (0001) in the normal direction is still present, but the $(10\bar{1}0)$ maximum in the rolling direction is more extended and instead a $(11\bar{2}0)$ maximum is developing in the rolling direction corresponding to a 30° rotation of crystals around the *c* axis. This feature has also been observed by Puig-Molina *et al.* (2003). Note that in the $(10\bar{1}0)$ and $(11\bar{2}0)$ pole figures of the recrystallized sample, there are slight deviations from orthorhombic symmetry (Fig. 2*c*). This feature is already visible in the diffraction image (Fig. 1*b*) and is attributed to limitations of grain statistics. If only texture were of interest, an

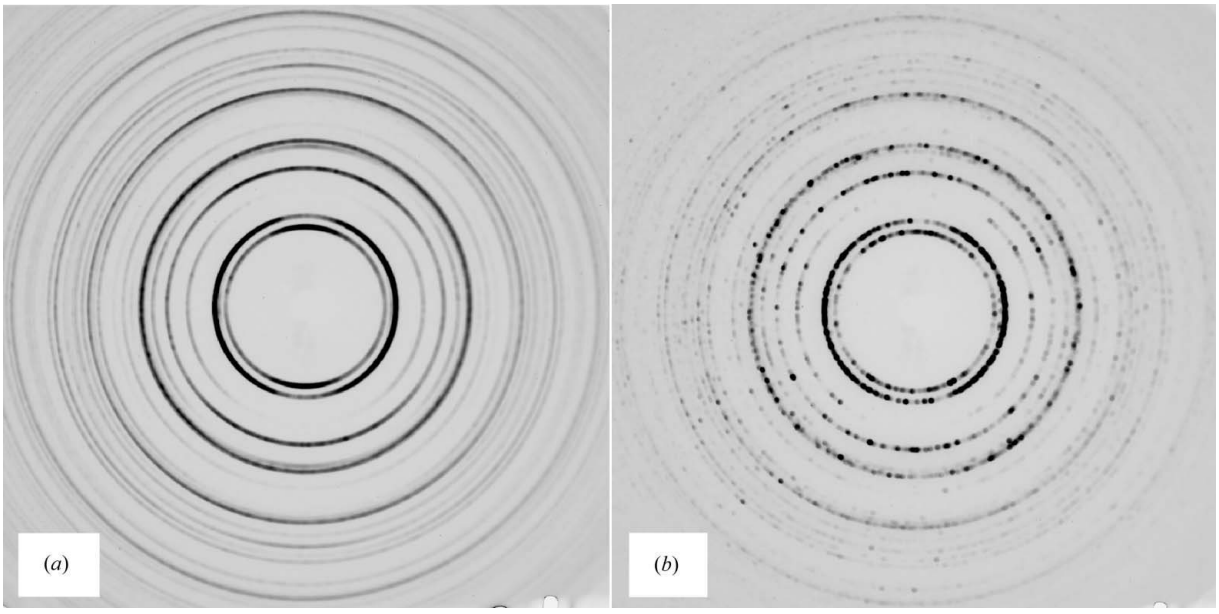

Figure 1
Synchrotron diffraction images of cold-rolled zirconium measured at ESRF beamline ID15 in a vacuum furnace at (*a*) room temperature and (*b*) 833 K with advanced grain growth.

oscillatory translation of the sample during data collection would have alleviated this problem, but in that case it would have been difficult to follow the nucleation and grain growth process, which was the goal of the experiment.

The Rietveld method combined with a WIMV texture algorithm provides a powerful new approach to investigating textured synchrotron images. For simple images, such as those presented here, the analysis is straightforward but not automatic, and we have not explored limitations caused by crystal symmetry and texture types. A sufficient number of *hkl* reflections is required, which favors low symmetry, large unit cells and high-energy X-rays. Clearly, the combination of several images taken in different orientations would improve the ODF resolution (Lonardelli *et al.*, 2005), but such a combination can often not be achieved. At this stage, the ODF analysis cannot be performed in real time, although real-time analysis may become possible in the future. The present method is an advance over previous methods that rely on sample rotation and mechanical filters, which discard a large part of the image information (Bunge *et al.*, 2003), and also over cumbersome intensity extraction from Debye rings, which is often impossible in materials with overlapping diffraction peaks (Wenk & Grigull, 2003).

6. Conclusions

Without rotating the sample, a quantitative three-dimensional orientation distribution can be obtained from a single two-dimensional diffraction image, without imposing sample symmetry. A modified WIMV algorithm is efficient for obtaining the ODF for minimal pole-figure coverage and the method can even be applied if grain statistics are not optimal. Compared with other diffraction methods (pole-figure goniometry, neutron diffraction, EBSD), synchrotron texture analysis is extremely fast and lends itself to dynamic studies at non-ambient conditions. Since the Rietveld method relies on crystal structure information, this method performs a direct texture correction for crystal structure refinements.

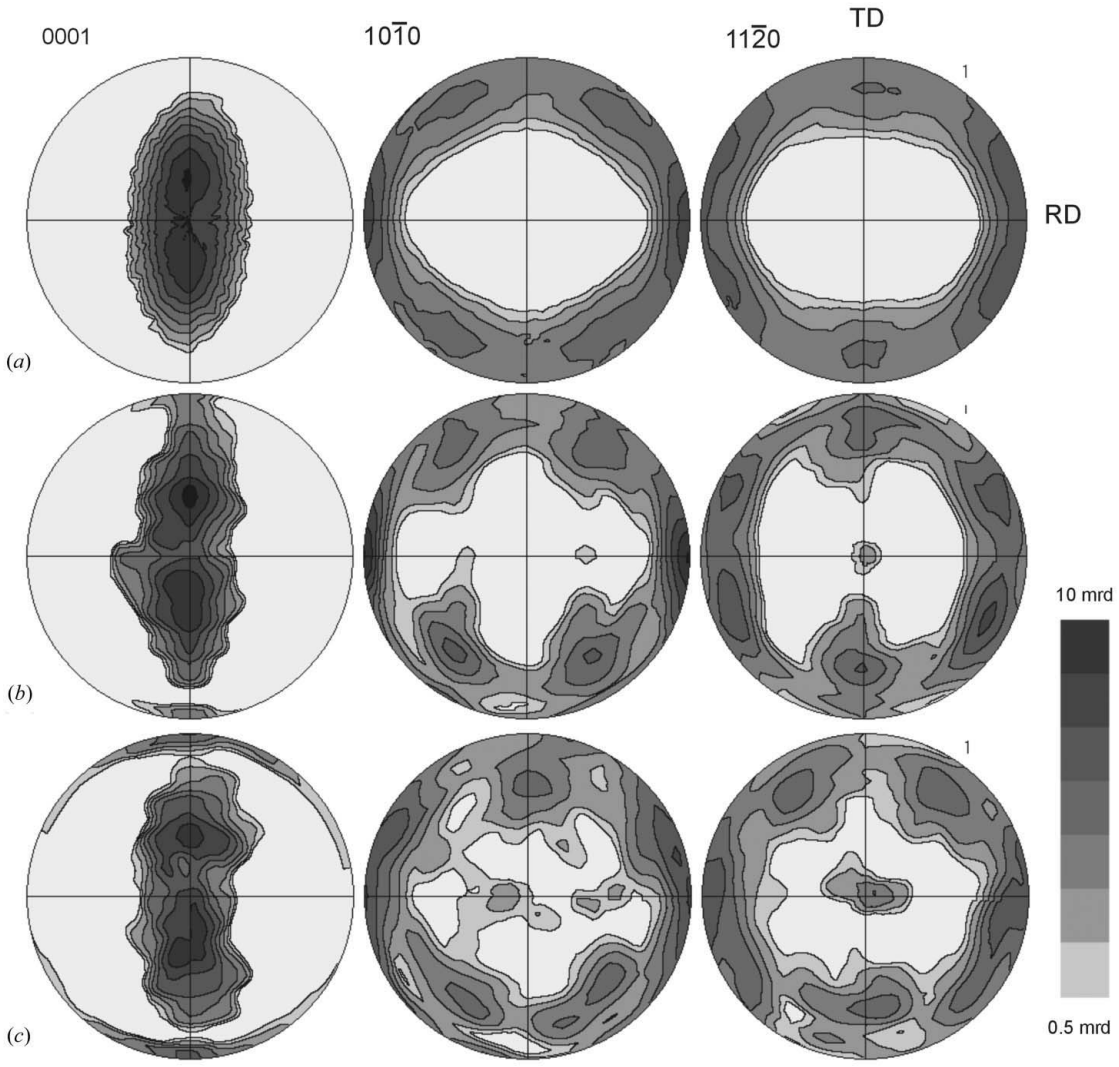

Figure 2
Pole figures recalculated from the ODF for rolled zirconium. Equal-area projection. The same logarithmic contour scale is used for all pole figures. (*a*) Sample measured with a conventional pole-figure goniometer (Cu $K\alpha$ radiation), (*b*) synchrotron X-ray measurements of the same sample at room temperature and (*c*) synchrotron measurements at 833 K. RD is the rolling direction; TD is the transverse direction; the normal direction is in the center.

The authors are appreciative for access to the facilities at beamline 15B at the ESRF. The research was supported by the NSF, CDAC and IGPP-LANL. Wah Chang, Oregon, kindly provided the zirconium sample. Suggestions by D. Chateigner were very helpful. HRW acknowledges generous hospitality at GFZ Potsdam, where part of this research was completed.

References

Bäckstrøm, S. P., Riekel, C., Abel, S., Lehr, H. & Wenk, H.-R. (1996). *J. Appl. Cryst.* **29**, 118–124.
Bunge, H. J., Wcislak, L., Klein, H., Garbe, U. & Schneider, J. R. (2003). *J. Appl. Cryst.* **36**, 1240–1255.
Hammersley, A. P. (1998). *FIT2D: V99.129 Reference Manual Version 3.1*. Internal Report ESRF-98-HA01, ESRF, Grenoble, France.
Heidelbach, F., Riekel, C. & Wenk, H.-R. (1999). *J. Appl. Cryst.* **32**, 841–849.
Lonardelli, I., Wenk, H.-R., Lutterotti, L. & Goodwin, M. (2005). *J. Synchrotron Rad.* In the press.
Lutterotti, L., Matthies, S., Wenk, H.-R., Schultz, A. S. & Richardson, J. W. Jr (1997). *J. Appl. Phys.* **81**, 594–600.
Matthies, S. & Vinel, G. W. (1982). *Phys. Status Solidi B*, **112**, K111–K114.
Pawlik, K. (1986). *Phys. Status Solidi B*, **134**, 477.
Puig-Molina, A., Wenk, H.-R., Berberich, F. & Graafsma, H. (2003). *Z. Metallkd.* **94**, 1199–1205.
Skrotzki, W., Kloeden, B., Tamm, R., Oertel, C.-G., Garbe, U. & Rybacki, E. (2003). *Textures Microstruct.* **35**, 163–173.
Wenk, H.-R. & Grigull, S. (2003). *J. Appl. Cryst.* **36**, 1040–1049.
Wenk, H.-R. & Heidelbach, F. (1998). *Bone*, **24**, 361–369.
Wenk, H.-R., Lonardelli, I., Pehl, J., Devine, J., Prakapenka, V., Shen, G. & Mao, H.-K. (2004). *Earth Planet. Sci. Lett.* **226**, 507–519.
Wenk, H.-R., Lonardelli, I. & Williams, D. (2004). *Acta Mater.* **52**, 1899–1907.
Wenk, H.-R., Matthies, S., Donovan, J. & Chateigner, D. (1998). *J. Appl. Cryst.* **31**, 262–269.